ISSN 1062-8738, Bulletin of the Russian Academy of Sciences: Physics, 2010, Vol. 74, No. 4, pp. 542–546. © Allerton Press, Inc., 2010.
Original Russian Text © O.V. Bespalova, I.N. Boboshin, V.V. Varlamov, T.A. Ermakova, B.S. Ishkhanov, A.A. Klimochkina, S.Yu. Komarov, H. Koura, E.A. Romanovsky, T.I. Spasskaya, 2010, published in Izvestiya Rossiiskoi Akademii Nauk. Seriya Fizicheskaya, 2010, Vol. 74, No. 4, pp. 575–579.

Neutron Shell Structure of ^{58,60,62,64}Ni Nuclei and Its Study within a Mean-Field Model with Dispersive Optical-Model Potential

O. V. Bespalova[a], I. N. Boboshin[a], V. V. Varlamov[a], T. A. Ermakova[a], B. S. Ishkhanov[a], A. A. Klimochkina[a], S. Yu. Komarov[a], H. Koura[b], E. A. Romanovsky[a], and T. I. Spasskaya[a]

[a] *Skobeltsyn Institute of Nuclear Physics, Moscow State University, Moscow, 119992 Russia*
e-mail: besp@sinp.msu.ru

[b] *Advanced Science Research Center, Japan Atomic Energy Agency, Tokai, Ibaraki 319-1195, Japan*

Abstract—Experimental single-particle energies and occupation probabilities for neutron states near the Fermi energy in ^{58,60,62,64}Ni nuclei were obtained from joint evaluation of the data on nucleon stripping and pickup reactions on the same nucleus. Degeneracy of the $2p_{3/2,1/2}$ and $1f_{5/2}$ subshells was demonstrated. The resulting data were analyzed within a mean-field model with dispersive optical-model potential. Good agreement was obtained between the calculated and experimental single-particle energies of the subshells.

DOI: 10.3103/S106287381004026X

INTRODUCTION

Single-particle representations are basic to an understanding of nuclear structure. A specific feature of the single-particle structure of $^{58, 60, 62, 64}$Ni nuclei is the closeness of the energies E_{nlj} of the $2p_{3/2}$, $1f_{5/2}$, and $2p_{1/2}$ subshells separated from the $1f_{7/2}$ subshell by a particle–hole energy gap that forms the magic number $N = 28$. Degeneracy of the $2p_{3/2}$, $1f_{5/2}$, and $2p_{1/2}$ subshells in the ^{58,60,62,64}Ni nuclei was theoretically predicted in [1] during calculations by the shell model with effective GXPF1 interaction for pf-shell nuclei. According to [1], the above subshells make up a unified state that may be treated as a degenerate pseudo-*s*–*d*-shell.

Experimental data on single-particle energies obtained from analysis of the data on nucleon stripping or pickup reactions do not usually allow closely spaced subshells to be discriminated, as the characteristic error of these data (20–30%) is larger than the subshell spacing. Joint evaluation of the data on nucleon stripping and pickup reactions on the same nucleus [2] (referred to below as the joint evaluation method) makes it possible to minimize systemic errors in determining the single-particle energies near the Fermi energy E_F and to reduce the total error of E_{nlj} values to 10% or so. These data allow the closely spaced subshells near E_F to be discriminated and may be an effective test for modern theoretical models.

In practice, consistent microscopic calculation of the single-particle structure of final nuclei involves appreciable difficulties. In [3], a semiempirical dispersion approach was elaborated to find the nuclear mean field, a unified field for positive and negative energies. This approach makes it possible to calculate single-particle energies, occupation probabilities, fragmentation widths, spectroscopic factors, spectral functions, root-mean-square radii of single-particle orbits, and data on scattering of nucleons from nuclei. In [4], a method for constructing nuclear mean field within the dispersion approach and the dispersive optical-model potential (DOP) were developed, aimed at describing and predicting the single-particle energies of nuclei. In this work, the method in [4] was used to analyze experimental data on E_{nlj} obtained by the joint evaluation method and applied to neutron states near E_F in ^{58,60,62,64}Ni nuclei.

EXPERIMENTAL

Single-Particle Energies and Occupation Probabilities for Neutron States of ^{58,60,62,64}Ni Nuclei

The idea of mutual correction of the data from the nucleon stripping and pickup experiments underlies the joint evaluation method [2]. The systemic errors in these experiments, which are partially due to incorrect absolute normalization of cross sections, are compensated for by introducing factors m^+ and m^-. These renormalize the spectroscopic forces S^+_{nlj} and S^-_{nlj} of the stripping and pickup reactions, respectively. In this approach, the sum rule is written as

$$m^+S^+_{nlj} + m^-S^-_{nlj} = 2j + 1, \quad (1)$$

and this relation is assumed to hold simultaneously for the three subshells nearest to E_F. The center of the single-particle fragment distribution is made to correspond to the single-particle energy.

Since spins and parities of the states of reaction product nuclei are often not determined experimentally, mutual correction of the nucleon stripping and pickup data involves the Monte Carlo exhaustion of all

Table 1. Experimental and calculated single-particle energies E_{nlj} (in MeV) and experimental occupation probabilities N_{nlj}^{expt} for neutron subshells in ^{58,60,62,64}Ni nuclei

Subshell	N_{nlj}^{expt}	$-E_{nlj}^{\text{expt}}$	$-E_{nlj}^{\text{DOP}}$	$-E_{nlj}^{\text{KY}}$	$-E_{nlj}^{\text{GXPF1}}$	$-E_{nlj}^{\text{RMFT}}$
			^{58}Ni			
$2p_{1/2}$	0.15(4)	8.54(81)	9.15	8.71	7.54	7.27
$2p_{3/2}$	0.28(3)	9.92(21)	10.31	10.62	9.61	8.89
$1f_{5/2}$	0.32(3)	10.53(28)	10.60	8.22	8.15	8.36
$1f_{7/2}$	0.89(2)	15.20(19)	15.14	15.13	15.54	17.29
$1d_{3/2}$	0.99(1)	19.82(9)	21.50	19.42		26.90
$\chi^2(N)$			0.28(5)	0.98(5)	1.66(4)	4.44(5)
			^{60}Ni			
$2p_{1/2}$	0.25(4)	8.17(19)	8.30	8.48	7.91	7.45
$2p_{3/2}$	0.48(6)	8.81(35)	9.69	10.37	10.01	9.11
$1f_{5/2}$	0.39(5)	9.20(24)	9.17	8.20	7.83	8.71
$1f_{7/2}$	0.98(2)	15.16(22)	15.12	14.96	15.24	17.41
$\chi^2(N)$			0.09(4)	0.80(4)	1.82(4)	0.85(4)
			^{62}Ni			
$1g_{9/2}$	0.04(4)	5.42(26)	5.40	5.69		3.49
$2p_{1/2}$	0.32(11)	7.62(63)	8.28	8.27	7.69	7.62
$1f_{5/2}$	0.47(12)	8.47(70)	8.93	8.20	8.07	9.10
$2p_{3/2}$	0.60(4)	8.85(30)	9.15	10.14	9.70	9.31
$\chi^2(N)$			0.30(4)	0.80(4)	0.38(3)	3.78(4)
			^{64}Ni			
$2d_{5/2}$	0.04(1)	2.65(3)	2.62	2.79		
$1g_{9/2}$	0.09(2)	5.56(13)	5.23	5.70		3.78
$2p_{1/2}$	0.42(1)	7.62(6)	7.98	8.06	7.47	7.82
$1f_{5/2}$	0.64(7)	8.72(60)	8.33	8.22	8.54	9.47
$2p_{3/2}$	0.78(1)	9.10(4)	9.01	9.92	9.39	9.52
$\chi^2(N)$			0.16(5)	0.36(5)	0.06(3)	2.82(4)

possible spins and parities [5]. In addition, the condition that the total number of nucleons is retained when residual interactions are included is imposed. As a result, the total error of the joint evaluation data on single-particle energies E_{nlj}^{expt} and occupation probabilities for single-particle orbits N_{nlj}^{expt} comprises the corrected error of the spectroscopic forces and the error due to lack of knowledge of the exact spin and parity values for the states.

The data on the levels of final nuclei in the neutron stripping and pickup reactions on ^{58,60,62,64}Ni nuclei were taken from the ENSDF database [6]. The E_{nlj}^{expt} and N_{nlj}^{expt} values were found using two criteria: the sum rule fulfillment error could not be larger than 10% and the deviation of the summed number of nucleons in all subshells from the numbers N and Z known for each nucleus could not be larger than unity (a change in the number of nucleons by a larger value would mean a change in the nucleus itself). The E_{nlj}^{expt} and N_{nlj}^{expt} values obtained for the neutron states of the ^{58,60,62,64}Ni nuclei are presented in Table 1. In parentheses, we see errors due to uncertainty of the spin and parity; the total errors are 10%. As follows from the results, the $2p_{3/2}$, $1f_{5/2}$, and $2p_{1/2}$ subshells lie within a rather narrow energy corridor about 1–2 MeV wide, and the corresponding occupation probabilities differ greatly from zero and unity. The values of E_{nlj}^{expt} and N_{nlj}^{expt} thus confirm the theoretically obtained degeneracy of the $2p_{3/2}$, $1f_{5/2}$, and $2p_{1/2}$ subshells in the ^{58,60,62,64}Ni nuclei.

Calculation within a Mean-Field Model with Dispersive Optical-Model Potential

In the dispersion approach, the mean field is complex. Its real and imaginary parts are connected by the

Table 2. Neutron DOP parameters for ^{58,60,62,64}Ni nuclei

	^{58}Ni	^{60}Ni	^{62}Ni	^{64}Ni
α_I	89.0	87.3	85.0	83.0
β_s	67.0	62.4	59.0	53.5
E_F	−12.9	−12.1	−8.6	−8.2
V_{so}	4.5	5.5	5.0	5.7
$V_{HF}(E_F)$	50.1	48.4	47.1	46.1
γ	0.44	0.45	0.43	0.44

Note: Values α_I are in MeV fm^3; E_F, V_{HF}, (E_F), and β_s are in MeV; V_{so} are in MeV fm^2; γ is a dimensionless parameter; $\beta_I = 0.7$ MeV; $E_0 = -3.0$ MeV; $r_{HF} = r_d = 1.28$ fm; $a_{HF} = a_d = 0.535$ fm; $r_s = 1.20$ fm; $a_s = 0.669$ fm; $r_{so} = 1.02$ fm; $a_{so} = 0.59$ fm.

dispersion relation in such a way that the real part of the locally equivalent DOP is a sum of the Hartree–Fock-type component V_{HF}, which depends weakly on the energy, and the dispersion component $\Delta V_{s,d}$, which depends strongly on the energy in the region near E_F. The dispersion component is calculated from the data on the imaginary part of the DOP and, like this part, it is divided into volume (subscript s) and surface (subscript d).

A DOP construction method was proposed in [4]. It was intended for calculating single-particle properties of nuclei, including unstable neutron-rich and neutron-deficient nuclei. The method does not require experimental data on the scattering of nucleons from the target nucleus of interest, since the necessary data on the imaginary part are taken from the available systematics of the global parameters of the potential of the traditional (nondispersive) optical model. In particular, we used the systematics in [7] to determine the neutron DOP of ^{58,60,62,64}Ni nuclei.

For example, we followed the procedure in [7] for fixing the radius and diffuseness parameters $r_{s,d}$ and $a_{s,d}$ of the imaginary part of the DOP, and r_{so} and a_{so} of the spin–orbit potential (the designations from [4] are used here and below). Two more energy dependence parameters of the imaginary part of the DOP were found using the systematics [7]: parameter α_I, defining the plateau height of the volume integral $J_I(E)$, was found by formula (5) from [4]; parameter β_s, defining the slope steepness of the volume integral $J_s(E)$, was found by formula (7) from [4]. The dependences $J_I(E)$ and $J_s(E)$ were approximated by expression (4) from [4] with $n = 4$ and $E_0 \neq E_F$. The variable parameters for the imaginary part of the DOP were thus β_I and E_0, which define the steepness and beginning of the $J_I(E)$ curve slope. The strength parameter V_{so} of the spin–orbit potential was also varied.

Energy E_F was defined as a half-sum of the energies E_{nlj}^{expt} of the subshells between which the occupation probability N_{nlj}, which approximates the experimental data, reaches the value 0.5. These subshells were $1f_{5/2}$ and $1f_{7/2}$ for ^{58,60}Ni, $1f_{5/2}$ and $2p_{3/2}$ for ^{62}Ni, and $1f_{5/2}$ and $2p_{1/2}$ for ^{64}Ni.

The parameters $V_{HF}(E_F)$ and γ, which characterize the energy dependence of the Hartree–Fock component of the DOP, were found from formulas (13) and (11) from [4]. To accomplish this, evaluated values $E_{1s_{1/2}}^{\text{ev}}$ were found using the experimental dependences $E_{1s_{1/2}}^{\text{expt}}(A)$ [8] and the results from calculations by the RMFT [9]. These varied linearly from −63 MeV for ^{58}Ni to −61.6 MeV for ^{64}Ni.

While searching for the optimum values of the radius and diffuseness parameters r_{HF} and a_{HF} of the DOP's Hartree–Fock component, we found that they could be equated to the respective parameters r_d and a_d from the systematics [7]. This was probably due to the optimum parameters being sought by fitting them to the experimental energies of the states near the nuclear surface. The r_{HF} and a_{HF} parameters found by fitting them to the energies of deep-lying states usually exhibit less pronounced sensitivity.

Finally, the values of only three parameters, β_I, E_0, and V_{so}, were determined by a grid search. The search was stopped upon reaching the minimum of the quantity

$$\chi^2 = \frac{1}{N}\sum\frac{(E_{nlj} - E_{nlj}^{\text{expt}})^2}{\Delta^2}, \qquad (2)$$

where N is the number of subshells near E_F, and $\Delta \approx 10\%$ is the error of E_{nlj}^{expt}. The neutron DOP parameters found for ^{58,60,62,64}Ni nuclei are presented in Table 2. As is evident from the Table 2, the values obtained for β_I and E_0 turned out to be identical for all Ni isotopes under investigation.

The energies E_{nlj}^{DOP} calculated with the DOP parameters that we obtained are presented in Table 1 and compared to the experimental data and energies calculated within the shell model with GXPF1 interaction [1] and RMFT [9], and with the KY potential [10]. The table also presents the corresponding χ^2 values. In parentheses, we find the numbers N of the subshells near E_F for which calculated energies are available. A comparison allows us to conclude that the calculations employing the GXPF1 interaction, the DOP and the KY potential, correspond to the values $\chi^2 < 1$. The best description of E_{nlj}^{expt} for ^{58,60,62,64}Ni nuclei in general is obtained with the DOP of this work. For example, the χ^2_{DOP} values are much smaller than unity, while the χ^2_{KY} values are close to unity for all isotopes, the χ^2_{MCSM} values are larger than unity for ^{58,60}Ni, and the χ^2_{RMFM} values are much larger than unity for ^{58,62,64}Ni. Figure 1 graphically shows the agreement of

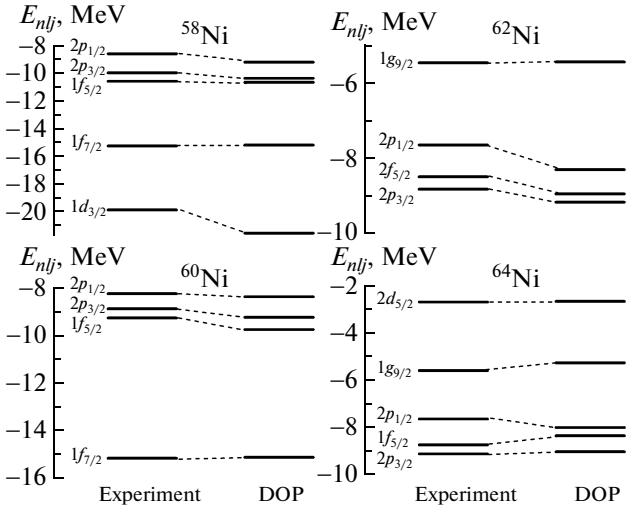

Fig. 1. Single-particle energies E_{nlj}^{DOP} (right) and E_{nlj}^{expt} (left) of the neutron subshells near E_F in ^{58,60,62,64}Ni nuclei.

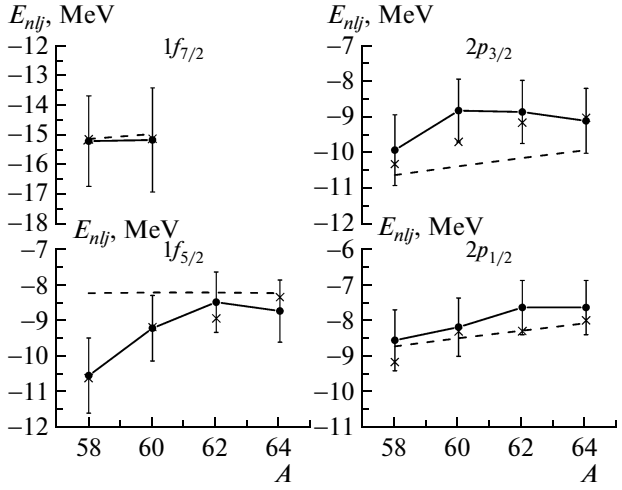

Fig. 2. Single-particle neutron energies E_{nlj} for the $2p$ and $1f$ states in ^{58,60,62,64}Ni nuclei. Dashed curves are energies E_{nlj}^{KY}, solid circles connected with a solid line are energies E_{nlj}^{expt}, and crosses are energies E_{nlj}^{DOP}.

the calculated values E_{nlj}^{DOP} and the experimental values E_{nlj}^{expt} obtained by the joint evaluation method. The dispersion approach, using the parameters found by the method in [4], allows the degeneracy of the $2p_{3/2}$, $1f_{5/2}$, and $2p_{1/2}$ subshells in ^{58,60,62,64}Ni nuclei to be described.

The mass dependences of energies E_{nlj}^{DOP}, E_{nlj}^{KY}, and E_{nlj}^{expt} of the $2p_{1/2,3/2}$ and $1f_{5/2,7/2}$ neutron subshells are compared in Fig. 2, where calculated energies E_{nlj}^{DOP} are seen to be in good agreement with the experimental data. When comparing E_{nlj}^{KY} and E_{nlj}^{expt}, we should bear in mind that the KY potential was selected on the basis of the data on the position of the maximum spectroscopic factor of the single-particle state fragments, while energies E_{nlj}^{expt} are the positions of the fragment distribution centroid. One reason for the difference between E_{nlj}^{KY} and E_{nlj}^{expt} could therefore be fragmentation of the single-particle state. The difference between E_{nlj}^{KY} and $E_{nlj}^{\mathrm{expt}}$is most pronounced for the $2p_{3/2}$ and $1f_{5/2}$ states. In addition, we may expect that the energy of the latter state can be affected by the energetically close $1f_{7/2}$ proton state, due to the $j_> - j_<$ interaction [11].

The imaginary part that is present in the mean field of the dispersion approach makes it possible to calculate various single-particle characteristics of the nucleus, particularly the occupation probability N_{nlj} for single-particle subshells. Probabilities N_{nlj} can be calculated using approximate expressions (see [3]). Here the difference of N_{nlj} from zero for $E_{nlj} > E_F$ is determined by the imaginary part of the DOP for $E < E_F$, and the difference of N_{nlj} from unity for $E_{nlj} < E_F$ is determined by the imaginary part of DOP for $E > E_F$. By way of example, Fig. 3 shows the calculated probabilities N_{nlj}^{DOP} for near-E_F neutron subshells in a ^{58}Ni nucleus, as compared to the experimental values N_{nlj}^{expt} obtained by the joint evaluation method. Calculations with the DOP yield slightly understated (by ≈0.1) results, as compared to N_{nlj}^{expt}, and yet they correctly describe the dependence $N_{nlj}^{\mathrm{expt}}(E_{nlj})$.

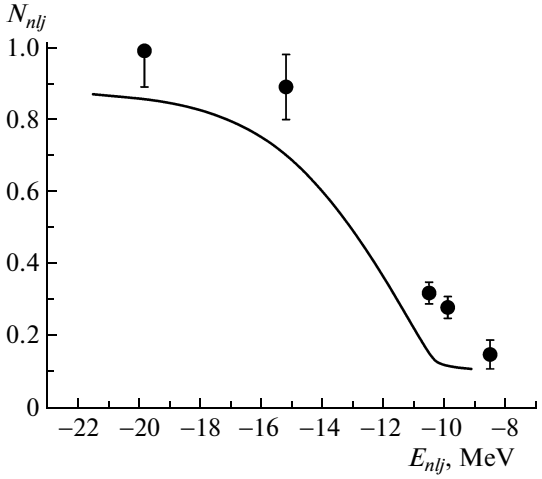

Fig. 3. Occupation probabilities N_{nlj}^{DOP} for neutron subshells near E_F in a ^{58}Ni nucleus, as compared to experimental values N_{nlj}^{expt}.

CONCLUSIONS

The results of this work are part of systematic studies of the single-particle structure of nuclei with mass numbers of 40 to 208. Experimental single-particle energies and occupation probabilities for single-particle neutron states in ^{58,60,62,64}Ni nuclei near E_F are found by joint evaluation of the data from the nucleon stripping and pickup reactions on the same nucleus. The values obtained for E_{nlj}^{expt} and N_{nlj}^{expt} demonstrate degeneracy of the $2p_{3/2}$, $1f_{5/2}$, and $2p_{1/2}$ subshells in these nuclei. Our investigations extend and refine modern concepts of the single-particle structure of nuclei and allow effective verification of modern theoretical models based on these concepts.

A mean-field model with dispersive optical-model-potential was used to analyze the E_{nlj}^{expt} and N_{nlj}^{expt} data. The DOP was constructed by the method in [4] and had only three variable parameters. Good agreement of E_{nlj}^{DOP} and E_{nlj}^{expt}, characterized by a χ^2, much smaller than unity, is obtained. The calculated occupation probabilities N_{nlj}^{DOP} for single-particle neutron states yield a qualitatively correct description the dependence $N_{nlj}^{\text{expt}}(E_{nlj})$.

ACKNOWLEDGMENTS

This work was supported by the Federal Agency for Science and Innovations, contract 02.740.11.0242, under the provisions of program 1.1, "Scientific Research Carried out by Teams of Scientific Educational Centers"; and by grant 02.120.21.485–NSh for the support of leading scientific schools.

REFERENCES

1. Honma, M., Otsuka, T., Brown, B.A., et al., *Phys. Rev. C*, 2002, vol. 65, p. 061301.
2. Boboshin, I.N., Varlamov, V.V., Ishkhanov, B.S., *Nucl. Phys. A*, 1989. vol. 496, p. 93.
3. Mahaux, C. and Sartor, R., *Adv. Nucl. Phys.*, 1991, vol. 20. p. 1.
4. Bespalova, O.V., Boboshin, I.N., Varlamov, V.V., et al., *Yadern. Fiz.*, 2009, vol. 72, no. 10, p. 1686 [*Phys. of Atomic Nuclei* (Engl. Transl.), 2009, vol. 72, no. 10, p. 1617].
5. Bespalova, O.V., Boboshin, I.N., Varlamov, V.V., et al., *Izv. Akad. Nauk, Ser. Fiz.*, 2008, vol. 72, no. 6, p. 896 [*Bull. Russian. Acad. Sci.* (Engl. Transl.), 2008, vol. 72, no. 6, p. 847].
6. http://www.nndc.bnl.gov/ensdf; http://www.cdfe.sinp.msu.ru/services/ensdfr.html
7. Koning, A.J. and Delaroche, J.P., *Nucl. Phys. A*, 2003, vol. 713, p. 231.
8. Volkov, S.S., Vorob'ev, A.A., Domchenkov, O.A., et al., *Yadern. Fiz.,* 1990, vol. 52, p. 1339; Vorob'ev, A.A., Dotsenko, Yu.V., Lobodenko, A.A., et al., *Yadern. Fiz.*, 1995, vol. 58, p. 1923.
9. Typel, S. and Wolter, H.H., *Nucl. Phys. A*, 1999, vol. 656, p. 331.
10. Koura, H. and Yamada, M., *Nucl. Phys. A,* 2000, vol. 531, p. 96.
11. Otsuka, T., Fujimoto, R., Utsuno, Y., et al., *Phys. Rev. Lett.*, 2001, vol. 87, p. 082502.